

BLIND OCEAN ACOUSTIC TOMOGRAPHY WITH SOURCE SPECTRUM ESTIMATION

S.M. JESUS AND C. SOARES

*SiPLAB-FCT, University of Algarve, Campus de Gambelas,
PT-8000-117 Faro, Portugal
E-mail: {sjesus,csoares}@ualg.pt*

Classic acoustic tomography uses controlled sound sources to probe the ocean for its physical properties. Instead, passive ocean acoustic tomography aims at using natural noise sources, such as wind induced noise, wave noise, or shipping noise with the scope of inverting for the ocean and/or bottom geophysical properties. Most studies found in the literature make use of ambient noise and sea surface wind generated noise, to invert bottom parameters in shallow water regions. Recently, another approach used shipping noise as illuminating signals to invert for water column parameters [Jesus et al., Conference on Acoustic Variability, Lercici (Italy), September 2002]. In that work, a focalization process was used to simultaneously invert known geometrical and unknown environmental parameters. In particular it was shown that known geometrical parameters such as source range and depth, and receiving array geometry, could be used as focus and out of focus indicators. During the focus periods, estimated water column parameters favorably compared to independently measured values. One of the difficulties found with the shipping noise was the low received power and the difficulty to determine a sufficient number of stable frequencies. In the present work, the received signal is used to deconvolve the source power, and thus obtain a full-spectrum weighting function for optimum frequency combination during the focalization process. Results obtained in the same ship noise data set have shown an certain improvement where a stable localization and inversion could be seen throughout the run.

1 Introduction

Ocean acoustic tomography (OAT) was introduced nearly 30 years ago by W. Munk but, to date, it has not become a standard technique in oceanic observation. Although, synoptic ocean temperature profiling in near real time appears extremely appealing for any oceanographer, OAT suffers from at least two main practical drawbacks. One is that in order to have a true synoptic ocean observation, the quantity of equipment in terms of source/receiver pairs is generally quite prohibitive in terms of cost, deployment needs and management or, at least, comparable to that required for classic oceanographic surveys. The other is that once the tomographic equipment has been installed the only information available (after inversion) are space integral temperature profiles between the several source/receiver pairs. Therefore, it is, in general, difficult to convince an oceanographer non addicted to acoustics, of the interest of using OAT instead of usual ocean sampling techniques.

As opposed to classic (active) OAT, in passive tomography natural noise sources in the ocean are used as input for inversion. Various forms of passive tomography have been proposed in the literature among which those that attempt to invert only for the bottom parameters in shallow regions making use of ambient noise directionality¹, sea surface wind generated noise^{2,3} or even aircraft noise⁴. Recently, passive OAT with shipping noise has been proposed also for estimating water column parameters⁵ or the full environment characterization^{6,7}. Both studies provided

meaningful water column SSP results but in the former a priori knowledge for all model parameters but the EOF coefficients was used while in the later a full-model inversion was performed throughout the data run. Such an inverse problem, where both the input signal and the propagation channel are unknown, is termed a blind deconvolution problem, and is common in areas such as wireless communications, geophysics and astronomy. This served as motivation to call the technique proposed in^{6,7} as Blind Ocean Acoustic Tomography (BOAT). In BOAT, a focalization technique, similar to that proposed by Collins⁸ for source localization, was implemented to simultaneously invert known geometrical and unknown environmental parameters. In particular, it was shown that known geometrical parameters such as source range, source depth, and receiving array geometry, could be used as *in focus* and *out of focus* indicators, in order to preclude convergence to false inverse solutions exhibiting high model fit values, the so called equivalent environmental models. Although the risk of converging to equivalent models always exists it was found that during the *in focus* periods estimated water column parameters favorably compared to independently measured values. This was particularly true when using assumed unknown deterministic signals, in a first attempt⁶, while for the shipping noise in⁷ the low received power and the difficulty to determine enough stable frequencies destroyed the result during several portions of the run. An attempt to improve the situation in the case of the ship noise inversion is presented in this paper, where the received signals are used to deconvolve the emitted source power, and thus obtain a full-spectrum weighting function for optimum frequency combination during the focalization process. This procedure avoids the requirement for an adhoc search of source frequencies, thus making the process fully automatic and near optimal in the sense of the minimum variance power spectrum estimation. The results obtained in the same ship noise data set have shown some degree of improvement, where a much more stable source localization and inversion could be seen throughout the run than in the previous results.

2 Experimental setup and data description

The data set shown in this paper was recorded during the INTIFANTE'00 sea trial that took place in October 2000, near the town of Setúbal, approximately 50 km south from Lisbon, in Portugal. An overall description of the sea trial can be found in⁹, whereas in this paper the interest will be focused only on Event 6. During this Event the signals received at the 16-hydrophone vertical line array (VLA) consisted on the noise radiated by the research vessel NRP D. Carlos I, cruising over a mildly range-dependent area up to 3.3 km range from the VLA. The NRP D. Carlos I is a 68 m overall length hydrographic ship with a gross displacement of 2800 tons. Her propulsion is obtained from a double helical diesel-electric engine with a total shaft power of 800 HP, attaining a maximum speed of 11 kn. It should be noted that NRP D. Carlos I was originally built for acoustic surveying so she is supposed to be a rather quiet ship. During Event 6, NRP D. Carlos I performed a triple bow shaped pattern at approximate ranges of 1.2, 2.2 and 3.3 km from the VLA as shown in figure 1.

A detailed bathymetry of the area was not available, but approximate bathy-

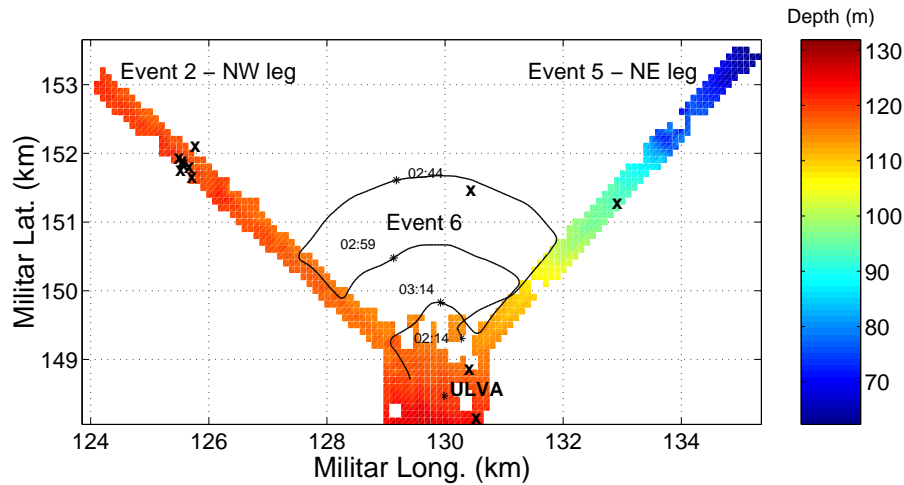


Figure 1. *INTIFANTE'00* sea trial Event 6 and site bathymetry. XBT casts locations are marked with **X** and **ULVA** denotes the VLA location.

metric profiles were made along both the NW and the NE legs (see figure 1). Therefore acoustic propagation between the ship and the VLA is assumed to be slightly downslope range-dependent to the NE, and progressively becoming range-independent, at 120 m water depth, to the NW. The maximum range-dependence is obtained for the 3.5 km range bow, with a maximum water depth difference of 20 m at the NE leg. A number of XBT casts were made during the sea trial at various times and locations as marked by the **X** signs on figure 1.

Ship's speed and heading, as obtained from GPS, is shown in figure 2, plots (a) and (b), respectively. It can be seen that mean ship speed was about 9 kn with several abrupt drops to 7 kn during the sharp ship turns along the trajectory. As it will be seen in the sequel, these speed drops will have a determinant impact in the ship radiated noise in terms of power spectrum and frequency extent in the useful band.

Acoustic signals received at the VLA exhibit a typical exponentially decreasing mean power spectra, characteristic of shipping noise with, however, a few strong lines at 250, 260 and 359 Hz and a coloured noise spectra in the band 500 to 700. On a preliminary analysis the maximum power frequency bins were extracted from a 8 s sliding window that gave a time varying number of bins between 1 and 4 as shown in⁷, and which is extremely poor for environmental inversion purposes in such a challenging environment. A second attempt, presented in this paper, steems from the idea that frequency information and source power may not be being used correctly in this case where the source signal is highly fluctuating both in time and frequency with a low signal-to-noise ratio (SNR), causing difficulties in selecting the right useful frequencies.

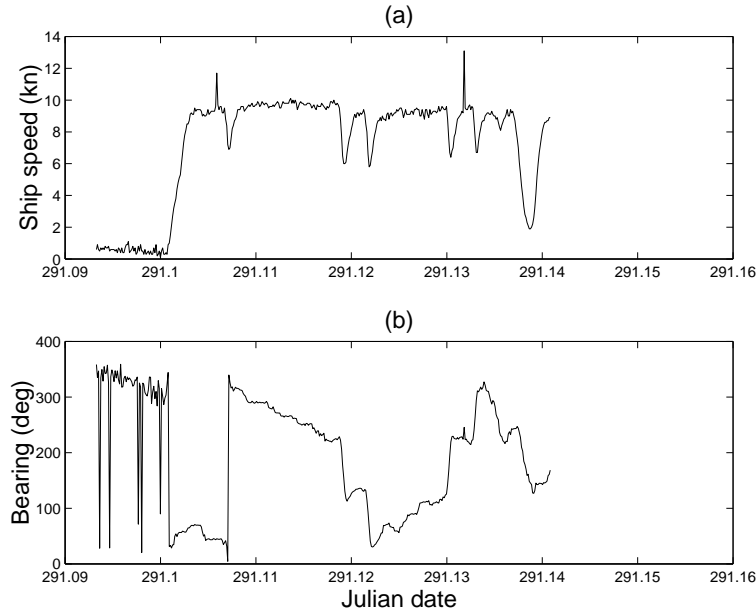


Figure 2. Event 6: GPS measured ship speed (a) and ship heading (b).

3 Multichannel source spectrum deconvolution

Let us assume that the L-sensor array-received signal at frequency ω can be written as¹⁰

$$\mathbf{y}(\omega, \theta_o) = \alpha(\omega)\mathbf{h}(\omega, \theta_o)s(\omega) + \mathbf{u}(\omega) \quad (1)$$

where $\mathbf{y} = [y(z_1), y(z_2), \dots, y(z_L)]^t$ and similar definitions hold for \mathbf{h} and \mathbf{u} , the replica model vector and the additive observation noise vector, respectively; $s(\omega)$ is the source spectrum at frequency ω and θ_o is a vector with the relevant parameters under estimation. The noise process \mathbf{u} is assumed to be uncorrelated from sensor to sensor and with random factor α . Note that random factor $\alpha = |\alpha| \exp(j\phi)$ is supposed to represent the channel random variations on the emitted signal between source and receiver and it is assumed space invariant but frequency dependent. For the design of optimal estimators it is useful to consider that α is zero-mean and Gaussian distributed.

Using data model (1), the broadband incoherent Bartlett processor has the following form¹⁰

$$P_{\text{inc}}(\theta) = \frac{\sum_{k=1}^K |s(\omega_k)|^2 \mathbf{h}^H(\omega_k, \theta) \mathbf{C}_{yy}(\omega_k) \mathbf{h}(\omega_k, \theta)}{\|\mathbf{H}(\theta)\mathbf{s}\|^2}, \quad (2)$$

where θ is the test parameter vector seeking the true value θ_0 , $\mathbf{h}(\omega_k, \theta)$ is the replica model vector taken at frequency ω_k and for test parameter θ , $\mathbf{C}_{yy}(\omega_k)$ is the data covariance matrix at frequency ω_k , K is the number of frequencies, $\mathbf{H}(\theta)$

is a matrix formed with all replica channel vectors \mathbf{h} along the main diagonal and $s(\omega_k)$ is the source amplitude at frequency ω_k , and \mathbf{s} is the source vector with entries $s(\omega_k)\alpha(\omega_k)$ for all K frequency bins. Equation (2) is optimum if the noise is spatially uncorrelated and the signal cross frequency correlations are zero. Another source of non-optimality is that in practice, the source emitted power $|s(\omega_k)|^2$ is unknown and a flat source spectrum is often assumed, leading to an equally weighted form of (2) where $|s(\omega_k)|^2 = 1$. This is a suboptimum processor, that is as far from the optimum case as the source power spectrum is non flat and the cross-frequency data correlations are different from zero which is seldom the case in practice. It is believed that this is the case for the data set of Event 6 where the ship noise spectrum is highly time-varying and non flat in general. The source power estimates $\hat{s}(\omega_k)$ were obtained with a Maximum Likelihood estimator (MLE) conditioned on the environmental parameter θ , of the form

$$\hat{s}(\omega_k) = \frac{\mathbf{h}^H(\omega_k, \theta)E[\mathbf{y}(\omega_k)]}{\mathbf{h}^H(\omega_k, \theta)\mathbf{h}(\omega_k, \theta)}. \quad (3)$$

The basic idea is to reach a better approximation of the source spectrum in the band used for inversion, thus relaxing the problem of frequency selection: if a low source power frequency is selected at a given time, it will be “correctly” assigned with a low source power estimate. Even in this case, computational limitations lead to the necessity of reducing the frequency sampling, thus another criterion was used to select the spectral components with smaller variance (in a given time frame). This is based on the assumption that the frequency bins with higher variance are more likely to contain only ambient and electronic noise. Thus if the received signal variance is estimated by

$$V_y(\omega, l) = \frac{1}{T} \sum_{t=1}^T [y_l(\omega, t) - \mu_y(\omega)]^2, \quad (4)$$

where $y_l(\omega, t)$ is the received signal on hydrophone k in time window snapshot t at frequency ω , T is the total number of time snapshots and $\mu_y(\omega)$ is an estimate of the mean of y_l in the same data window. The frequency components with the lower variance are those that maximize the functional

$$v(\omega) = \frac{L}{\sum_{l=1}^L V_y(\omega, l)} \quad (5)$$

where the summation is calculated over the L hydrophones. As an example, applying this criteria to a 16 s duration data window at julian time 291.125 gave the results shown in figure 3: spectrogram in (a) and minimum variance selection in (b).

4 Baseline model and data inversion

4.1 The baseline model

An important step towards a successful data inversion relies on the choice of a suitable environmental model. There was no extensive oceanographic or geoacoustic

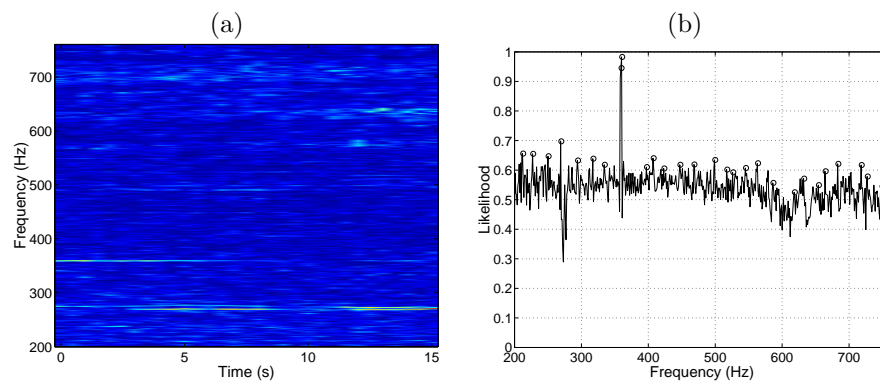


Figure 3. *INTIFANTE'00* sea trial, event 6, 16 s data window for hydrophone 8 at Julian time 291.125: spectrogram (a) and selected frequency bins for inversion using the minimum variance criterion (b).

survey concerning the area of Event 6. Therefore, as in a previous work⁶, identical generic assumptions based on archival data were adopted, giving rise to a range-independent baseline model with a 119 m depth waveguide with a mean downward refracting profile described by the two first EOF's drawn from a series of XBT's taken at different locations in space and time (see **X** signs in figure 1). Geoacoustic characteristics were empirically drawn from geological tables where the bottom was formed by a "fine sand" 4 m thick sediment layer with a constant compressional speed c_s , a compressional attenuation $\alpha_s=0.8$ dB/ λ and a density $\rho_s=1.9$ g/cm³ over a half space subbottom characterized by c_b , $\alpha_b = 0.8$ dB/ λ and $\rho_b = 1.9$ g/cm³. A focalization procedure carried out in the range independent area of the NW leg gave the estimates $c_s = 1556$ m/s and $c_b = 1657$ m/s for the compressional speeds of the sediment and bottom, respectively. These values were included in the baseline model for inverting the data of Event 6.

4.2 Data inversion

Data inversion was carried by a Matched-Field based optimization procedure using the C-SNAP forward model¹¹ and a Genetic Algorithm developed by Fassbender¹². The objective function is that given in (2) with the source amplitudes from (3). The covariance matrices were computed from 16 s duration time observations that were divided into segments of 1 s resulting in an average of 16 outer products at each frequency. The search parameters, respective search intervals and discretization steps are shown in table 1. Each inversion was carried out using three independent populations of 80 individuals each and 40 generations. The crossover and mutation probability were respectively set to 0.7 and 0.008. Each population was initialized using the solution obtained in the previous inversion: 30% of the individuals were initialized randomly in an interval with 10% of the search interval length with center at the best individual obtained in the previous iteration. This modified procedure lead to a faster convergence to the solution since the ship was moving

| Symbol | Unit | Search interval | | Steps |
|------------|------|-----------------|------|-------|
| | | min | max | |
| α_1 | m/s | -20 | 20 | 64 |
| α_2 | m/s | -20 | 20 | 64 |
| sr | km | 0.5 | 3.5 | 128 |
| sd | m | 1 | 10 | 32 |
| rd | m | 85 | 95 | 32 |
| θ | rad | -0.03 | 0.03 | 32 |

Table 1. Focalization parameters and search intervals: EOF1 (α_1), EOF2 (α_2), source range (sr), source depth (sd), receiver depth (rd), VLA tilt (θ)

in radial paths around the array and the environment was changing slowly over time. The inverted parameters can be divided in three groups: in the first group

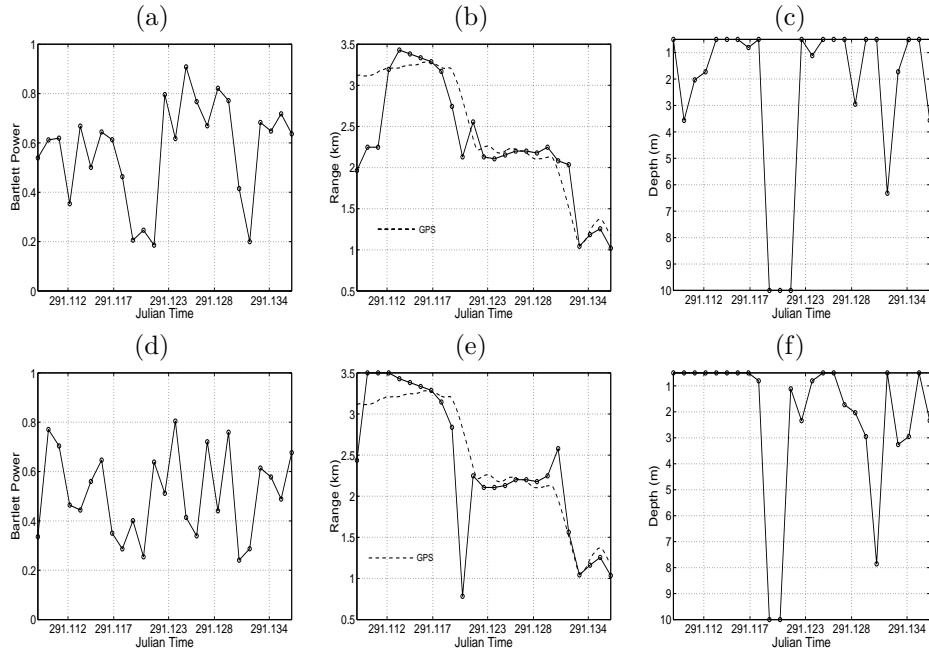


Figure 4. Focalization results for Event 6 - leading parameters with source amplitude estimation: Bartlett power (a), source range (b)[the dashed line is the GPS measured source-receiver range] and source depth (c); without source amplitude estimation: Bartlett power (a), source range (b)[the dashed line is the GPS measured source-receiver range] and source depth (c).

there are the leading geometric parameters such as source range and source depth; the second group has the least important parameters, that were included in the search to allow model adaptation to the data (focalization), such as array tilt,

sensor depth and other bottom parameters (held fixed during Event 6) and in the last group there are the desired output parameters as the EOF coefficients α_i , that provide the final result. The results obtained for the leading geometric parameters plus the Bartlett power are shown in figure 4 and the reconstructed temperature profiles, with the estimated EOF coefficients, in figure 5. When comparing the

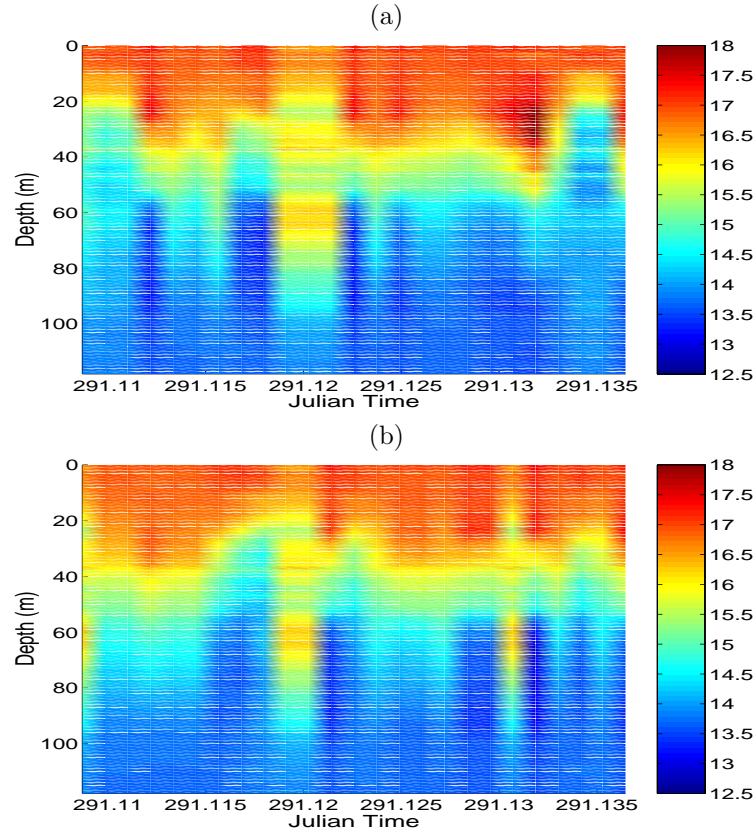


Figure 5. Focalization results for Event 6 - output temperature profile estimate: with source amplitude estimation (a) and without source amplitude estimation (b).

results obtained with source amplitude estimation (a) – (c) and those obtained without amplitude estimation (d) – (f) the following differences can be noted: *i*) no estimation drops exist anymore on the source-receiver range estimate as the ship turns while the estimated curve closely follows the GPS source range curve [plot (b)]; *ii*) the Bartlett power curve that, to some extent indicates model fit, is more stable over time in case (a) than in case (d) with still a few low values concentrated at the ship turn points; *iii*) these drops at the ship turning points are accompanied with mis-estimated source depth in curve (c) where values drop well below the expected estimate for a surface ship. So, a close inspection of these curves

can let us expect slightly better environmental estimate specially after the larger bow run, with only two exceptions: between times 291.119 and 291.122 and at a short interruption at time 291.132. Indeed, these expectations are verified when inspecting figure 5, in plot (a) using the source amplitude estimation procedure and in plot (b), without source amplitude estimation as obtained in⁷, for comparison.

5 Conclusion

Ocean tomography with sound sources of opportunity has been a longely sought dream for acoustic oceanographers. Preliminary results were obtained in⁷ using a technique called BOAT, in a ship radiated noise data set collected off Portugal during the INTIFANTE'00 sea trial. As opposed to other passive inversion techniques, that use analytical or partial model inversions, BOAT uses a full model parameter focalization, including environmental unknown as well as geometric partially known parameters. The coherence of the geometric parameter estimates was used as indicator of the convergence of the inversion to a “focused” estimate of the environment. It was found that this procedure performed relatively well in part of the data set when the ship was steaming at full speed in a benign environment. At low speed, during ship turns and when there was a significant mismatch between the true and the assumed environment, there was a clear loss of convergence and the estimates were erratic. These portions of the run were clearly indicated as “out of focus” by the geometric parameter estimates. One of the problems associated with these dropouts was a lack of frequency power support of the received ship noise at the receiving array. This paper presented an alternative method for providing a coherent estimate of the source radiated power through a multichannel deconvolution maximum likelihood (ML) based approach. The results show that inserting the ML estimated source power in the Bartlett power estimator, used as objective function in the inversion search algorithm, clearly provided an adaptive frequency weighting function that gave superior results than the previous method. In particular, it was found that the dropouts in the source range estimates have disappeared and the model fit is more stable than previously. It might be difficult to see a net improvement on the final estimated temperature profiles due to the still highly variable thermocline on a obviously too short run time of less than one hour. Therefore the proposed technique can be seen as an improvement to BOAT changing adhoc frequency selection into a fully automated procedure in presence of low or highly frequency and/or amplitude dispersed power sources. Validation of the BOAT technique, as a whole, requires longer runs of hours and days where it might be able to evaluate longer term oceanographic variations trends, before a final opinion can be formulated.

Acknowledgments

This work was supported by FCT, Portugal, under projects INTIMATE (2/2.1/MAR/1698/95), ATOMS (PDCTM/P/MAR/15296/1999) and TOM-PACO. The authors are also in debt to the crew of NRP D. Carlos I of the Instituto Hidrográfico, Lisbon, Portugal that made the sea trial successful.

References

1. Carbone N.M., Deane G.B. and Buckingham M.J., "Estimating the compressional and shear wave speeds of a shallow water seabed from the vertical coherence of ambient noise in the water column", *J. Acoust. Soc. America*, **103**(2), 801–813, (1998).
2. Harrison C.H. and Baldacci A., Bottom Reflection Properties by Inversion of Ambient Noise, *Proc. Sixth of European Conf. on Underwater Acoust., ECUA '02*, pp. 471-476, Gdansk, Poland, June (2002).
3. Harrison C.H.", The Influence of Noise and Coherence Fluctuations on a new Geo-Acoustic Inversion Technique, *Impact of Littoral Environment Variability on Acoustic Predictions and Sonar Performance*, ed. Pace and Jensen, pp.139-146, Kluwer, September (2002).
4. Buckingham M.J. and Giddens E.M. and Pompa J.B. and Simonet F. and Hahn T.R., A Light Aircraft As a Source of Sound for Performing Ge-Acoustic Inversion of the Sea Bed, *Proc. of Sixth European Conf. on Underwater Acoust., ECUA '02*, pp. 465-470, Gdansk, Poland, June (2002).
5. De Marinis E., Gasparini O., Picco P., Jesus S.M., Crise A. and Salon S., "Passive Ocean Acoustic Tomography: theory and experiment", *Proc. of Sixth European Conf. on Underwater Acoust., ECUA '02*, pp. 497-502, Gdansk, Poland, June, (2002).
6. Jesus S.M., Coares C., Onofre J. and Picco P., Blind Ocean Acoustic Tomography: Experimental results on the INTIFANTE'00 data set, to appear in *Proc. of European Conf. Underwater Acoust.*, pp.9-18, Gdansk, Poland, June (2002).
7. Jesus S.M., Soares C., Onofre J, Coelho E. and Picco P., Experimental testing of the Blind Ocean Acoustic Tomography concept, *Impact of Littoral Environment Variability on Acoustic Predictions and Sonar Performance*, ed. Pace and Jensen, pp.433-440, Kluwer, September (2002).
8. Collins M.D. and Kuperman W.A., Focalization: Environmental focusing and source localization, *J. Acoust. Soc. America*, **90**(3), 1410–1422, (1991).
9. Jesus S.M, Coelho E., Onofre J, Picco P, Soares C. and Lopes C., The INTIFANTE'00 sea trial: preliminary source localization and ocean tomography data analysis, *Proc. of the MTS/IEEE Oceans 2001*, Honolulu, Hawaii, USA, November (2001).
10. Soares C. and Jesus S.M., Broadband Matched-Field Processing: coherent and incoherent approaches, *Journal of the Acoustical Society of America*, **113**(5), pp. 2587-2598, (2003).
11. Ferla C.M., Porter M.B. and Jensen F.B., C-SNAP: Coupled SACLANTCEN normal mode propagation loss model, SACLANTCEN Undersea Research Center, Memorandum SM-274, La Spezia, Italy, (1993).
12. Fassbender T., Erweiterte Genetische Algorithmen zur globalen Optimierung multimodaler Funktionen, Diplomarbeit, Ruhr-Universität Bochum, (1995)